

Investigation of Mass Transfer on Single Droplets for the Reactive Extraction of Zinc with D2EHPA

Mehmet Yücel Altunok

BASF AG – Process Development, Henkelstr. 67, Düsseldorf D-40589, Germany

Murat Kalem

Bayer Technology Services GmbH, Leverkusen D-51368, Germany

Andreas Pfennig

AVT - Thermal Process Engineering, RWTH Aachen University, Wüllnerstr. 5, Aachen D-52062, Germany

DOI 10.1002/aic.12680

Published online June 16, 2011 in Wiley Online Library (wileyonlinelibrary.com).

Investigations of mass transfer behavior with the standard test system of the European Federation of Chemical Engineering (EFCE) for the reactive extraction zinc + D2EHPA (di(2-ethylhexyl) phosphoric acid) were carried out. Experiments were performed with single droplets in a mass transfer cell on lab-scale. In the experiments, contact time for the mass transfer between droplets and continuous phase, concentrations of zinc, D2EHPA and sulfuric acid, diameter of droplets and hole-diameter of sieve trays were varied. These experimental results show a systematic investigation of single droplet mass transfer behavior for the standard test system of the EFCE for the reactive extraction of zinc with D2EHPA. In the mass transfer model reported here, all transient effects are considered with an instability parameter, which was determined through experiments in a mass transfer cell. The simulation results with obtained instability parameters are in a good agreement with the experimental results.

© 2011 American Institute of Chemical Engineers *AIChE J.* 58: 1346–1355, 2012

Keywords: reactive extraction, mass transfer, mass-cell, simulation, extraction columns, standard test system, zinc + D2EHPA

Introduction

The performance of an extraction column is chiefly characterized by three phenomena, namely are mass transfer, fluid dynamics and droplet population behavior. Because of the strong interaction between these three phenomena, modeling-based design of extraction columns is not trivial. For reactive extraction systems, modeling is even more complex

due to the additional chemical reactions on top of the physical phenomena, the multicomponents behavior and the nonidealities resulting from the electrolytic nature of the ionic mixtures. Thus, often mixer-settler-equipment is used for industrial practices of reactive extraction.¹ This ensures a reliable design and operation based just on the equilibrium data, even though for the same extraction efficiency much smaller extraction columns would be required as compared to mixer-settler equipment.

A newly developed design method for pilot-plant scale columns is based on lab-scale experiments.^{2–4} Experiments in lab-cells run fast and are performed with small amounts of original substances. Based on the results of such lab-scale

Correspondence concerning this article should be addressed to A. Pfennig at andreas.pfennig@avt.rwth-aachen.de.

experiments, parameters describing sedimentation, coalescence, drop breakage and mass transfer into or from the droplets can be determined. The goal of this approach is the replacement or at least minimization of experiments on pilot-plant scale with appropriate simulations based on the lab-scale experiments. The basics of the approach concerning replacement of pilot-plant experiments with the simulations based on experiments in lab-scale go back to the 1980's. The first successful realization of this concept from the lab-to pilot-plant scale for nonreactive systems was achieved by Henschke³ at AVT, RWTH Aachen University.

The transfer of single-droplet behavior from the lab-scale to the column behavior in pilot-plant-scale, taking into account of effects like swarm behavior, fluid dynamics, axial and radial mixing and holdup, can be realized either by a modeling based on averaged characterization (e.g., via Sauter diameter) or based on a detailed consideration of droplet-population behavior. Weaknesses of the methods based on averaged data have been discussed further for physical extraction systems.^{5–10} As an alternative, the droplet population balances can be solved, where the droplet distribution for each height-segment in a extraction column is calculated accounting for the interaction of hydrodynamics, coalescence, splitting and mass transfer.

A direct solution of the droplet-population balances without chemical reactions has been performed recently by Attarakih,¹⁰ Attarakih et al.,¹¹ and Schmidt et al.¹² An alternative way to solve the drop-population balances also for complex systems is the ReDrop (representative drops) algorithm.^{2–4} In the ReDrop algorithm, individual drops are followed along their way through an extraction column. This simple and efficient way to solve drop-population balances, taking, e.g., lifetime of the drops as well as reactions into account, can be regarded as a Monte-Carlo integration of the balance equations. ReDrop has been applied to describe accurately the transient and steady-state behavior of pulsed columns with sieve trays, regular and random packings.^{3,13–15} The agreement with results of pilot-plant scale experiments is excellent also for a technical system with contaminations as reported by Weber et al.¹⁶ New research targets focus on the extension of ReDrop to the reactive extraction.^{17–19}

For the simulations with the ReDrop algorithm, experiments with single droplets in lab-cells are performed, to characterize the physical phenomena: fluid-dynamic, mass transfer, coalescence and splitting. In this work, experiments with single droplets in a mass transfer cell have been carried out in order to obtain the parameters needed for the physical description of mass transfer behavior of the reactive test system zinc + D2EHPA. The fluid-dynamic behavior of the standard test system for the reactive extraction of zinc with D2EHPA has recently been published by Kalem et al.²⁰

For the experimental investigations the standard test system of the European Federation of Chemical Engineering (EFCE) for the reactive extraction (zinc + water) in the aqueous phase and (D2EHPA + isododecane) in the organic phase were used. The physical properties of the standard test systems of EFCE have been well investigated. Therefore the standard test systems are convenient for comparison of extraction apparatus.^{21,22} The physical properties of the zinc-D2EHPA system have been used as reported by the EFCE.²²

D2EHPA is known to be in monomeric form in aromatic diluents and in dimeric form in aliphatic diluents where the following reaction occurs



The dimerization constant of D2EHPA in heptane is given as $10^{4.7}$ by Hancil et al.²³ D2EHPA is an interfacially active cation exchanger. The diethyl hexyl chain of D2EHPA is lipophilic and soluble in organic phases whereas the ionic hydrogen group is highly hydrophilic. D2EHPA extracts one zinc ion (Zn^{2+}) from an aqueous phase against two H^+ ions



Bars indicate components in the organic phase. The stoichiometric coefficients of the equilibrium reaction have been determined with FTIR slope analysis at low zinc concentrations and were used here as reported by Sainz-Diaz et al.,²⁴ Bart and Slater,²² and Bart.²⁵

Modeling of Mass Transfer into the Droplets

The theory for the modeling of the mass transfer into the droplets is based on the solution for the transient diffusion in a rigid sphere of the Newman-model^{26,27} with the assumption that the transport resistance in the continuous phase is negligible. Newman describes the time dependant average concentration in a droplet with

$$\frac{y(t) - y_I}{y_0 - y_I} = \frac{6}{\pi^2} \sum_{n=1}^{\infty} \frac{1}{n^2} \exp[-(n\pi)^2 Fo_d] \quad (3)$$

$y(t)$ is the mass concentration of transfer component at a given time t , y_0 is the initial zinc concentration in the organic droplets, y_I is the concentration at the interface and Fo_d is the Fourier-Number, which is dependent on the diffusion coefficient (D_d) and the droplet diameter (d).

The Newman-model^{26,27} has been applied to spherical droplets with inner circulations by Kronig and Brink²⁸ with the help of the approximated internal flow profile, which has been derived from Hadamard²⁹ and Rybczynski.³⁰ With increasing droplet diameter, circulations occur inside the droplets. These internal motions of droplet improve the mass transfer. Thus Kronig and Brink²⁸ introduce an effective diffusion coefficient with an enhancement factor (B)

$$D_{\text{eff}} = BD_d \quad (4)$$

where B is 2.5 for droplets with inner circulation and 1 for rigid spheres. Kronig and Brink²⁸ assume a laminar-flow regime inside the droplet, whereas Handlos and Baron³¹ assume a turbulent profile and thus introduce a new effective diffusion coefficient

$$D_{\text{eff}} = \frac{v_{\infty} d}{2048(1 + \frac{\eta_d}{\eta_c})}, \quad (5)$$

where v_{∞} is the sedimentation velocity of a single droplet. d is the droplet diameter, η_d is the viscosity of the droplet phase

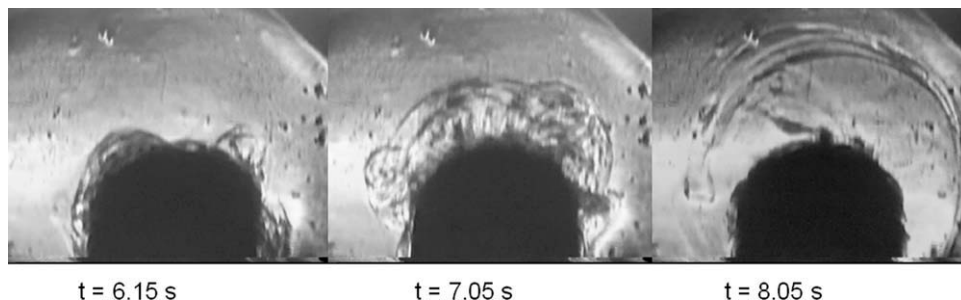


Figure 1. Instabilities at the interface of the zinc-D2EHPA system (Altunok¹⁹): $d_d = 4$ mm, $T = 20^\circ\text{C}$, $w_{\text{zinc}} = 500$ ppm in distilled water, $w_{\text{D2EHPA}} = 10$ wt % in isododecane, ($t = 0$ s: droplet formation).

and η_c is the viscosity of the continuous phase. Interestingly Handlos and Baron define D_{eff} independent of the physical diffusion coefficient D .

The models of Kronig and Brink²⁸ and of Handlos and Baron³¹ are based solely on molecular diffusion and fully established internal circulation inside the droplets, which underestimate the mass transfer rate by a factor of up to 10, as compared to experimental results. The reason for the larger mass transfer in reality could be explained by turbulences at the interface. Transient effects at interfaces improve the mass transfer and can occur in regular form, like Marangoni-convections, or in irregular form as reported by Sawitowski,³² Pfennig,³³ and Yurtov.³⁴ To illustrate this effect, Figure 1 shows the experimental results of Altunok¹⁹ at the interface of an organic droplet in the continuous phase. The organic droplet with a diameter of 4 mm consists of isododecane (90 wt %) and D2EHPA (10 wt %) and the aqueous phase of water and 500 ppm zinc. The experiments were carried out at a constant temperature of 20°C . The set up of the experiments is reported by Altunok.¹⁹ These results show how the interface is getting more instable because of strong turbulences, which are induced by the mass transfer.

A new approach for the modeling of the D_{eff} has been reported by Henschke and Pfennig,^{35,36} who describe the effective diffusion coefficient with a newly introduced instability parameter C_{IP} , which takes transient effects into account

$$D_{\text{eff}} = D_d + \frac{v_\infty d}{C_{\text{IP}}(1 + \frac{\eta_d}{\eta_c})} \quad (6)$$

C_{IP} is a substance specific constant and takes into account all transient effects through the diffusion, the convection, the turbulence caused by fluid dynamics, interfacial tension and the mass transfer including the contamination effect. The main advantage of this approach is that C_{IP} can be determined just with a single experiment, whereas fluid dynamic, droplet diameter and thermo-physical properties of the phases at the desired temperature and desired concentration range have to be taken into account.

The sedimentation velocities (v_∞) of the zinc-D2EHPA system were measured in a separate lab-cell. All relevant results of sedimentation behavior of the zinc-D2EHPA system have been reported by Kalem et al.²⁰

The time dependence of the concentration on the droplets is given as reported by Henschke and Pfennig³⁵ as

$$y^+ = \frac{y^* - y(t)}{y^* - y_0} = \frac{6}{\pi^2} \sum_{n=1}^{\infty} \frac{\exp[-(n\pi)^2 Fo^t]}{n^2} \quad (7)$$

where y^* is the mass concentration after the equilibrium has been reached ($y(t \rightarrow \infty) = y^*$). The approximate solutions of Eq. 7 are

$$y^+ = 1 - \frac{6}{\sqrt{\pi}} \sqrt{Fo^t} + 3.0 Fo^t \text{ for } Fo^t < 0.1584 \quad (8)$$

and

$$y^+ = \frac{6}{\pi^2} \exp(-(\pi)^2 Fo^t) \text{ for } Fo^t \geq 0.1584, \quad (9)$$

which give a solution of Eq. 7 with a deviation of less than 0.1%. Fo^t , the time dependent Fo -Number, is considered as the mass transfer coefficient by physical diffusion and convection

$$Fo^t = \frac{D_{\text{eff}} t}{(d/2)^2} \quad (10)$$

For the calculation of D_{eff} are the diffusion coefficients at infinite dilution (D_{ij}^0) are

required, which were estimated according to Wilke and Chang³⁷ model

$$D_{ij}^0 = 7.4 \times 10^{-8} \frac{T \sqrt{\varphi_j M_j}}{\eta_j v_i^{0.6}}, \quad (11)$$

where T is the temperature in K, φ is the dimensionless association factor, M is the molar mass, η is the dynamic viscosity in mPa.s and V is the molar volume here in cm^3/mol to become D_{ij}^0 in cm^2/s .^{*} The physical properties of components were taken from the EFCE.²² The diffusion coefficient of the zinc-complex in isododecane was calculated with the Darken³⁸ model

$$D_{ij} = (D_{ji}^0 x_i + D_{ij}^0 x_j) \Gamma_{ij}, \quad (12)$$

where the thermodynamic factor Γ_{ij} takes the deviation from an ideal mixture behavior into account

$$\Gamma_{ij} = \delta_{ij} + (x_i \frac{\partial \ln \gamma_i}{\partial x_j})_{T,p,x_k,k \neq j=1 \dots N-1} \quad (13)$$

^{*}The Equation of Wilke and Chang does not conform to SI-Units.

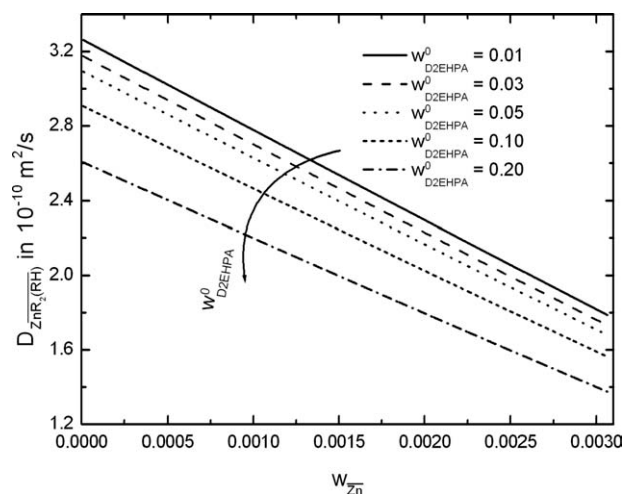


Figure 2. Diffusion coefficients of zinc-D2EHPA complex (Altunok¹⁹).

δ_{ij} is the Kronecker delta, with δ_{ij} ($i = j$) = 1 and δ_{ij} ($i \neq j$) = 0. The nonideality of the organic phase was calculated with the Hildebrand-Scott model by considering of Flory-Huggins correction term as reported by EFCE²²

$$\ln \gamma_i = \frac{V_i}{RT} (\delta_i - \bar{\delta})^2 + \ln \left(\frac{V_i}{V_m} \right) + 1 + \frac{V_i}{V_m}. \quad (14)$$

$\bar{\delta}$, the average solubility parameter, is defined as

$$\bar{\delta} = \frac{1}{V_m} (V_{ISO} \delta_{ISO} + \sum_{k=1}^2 \frac{c_k}{c_{tot}} (V_k \delta_k - V_{ISO} \delta_{ISO})), \quad (15)$$

where V_m is the average molar volume

$$V_m = \frac{c_{R_2H_2}}{c_{tot}} (V_{R_2H_2} - V_{ISO}) + \frac{c_{ZnR_2RH}}{c_{tot}} (V_{ZnR_2RH} - V_{ISO}) + V_{ISO} \quad (16)$$

The Hildebrand-Scott parameter δ_i , the molar mass M_i and the molar volume V_i of the components were used as reported by Bart and Slater.²² The final equations for calculation of the activity coefficient of D2EHPA and zinc-D2EHPA complex are

$$\gamma_{R_2H_2} = \frac{\exp \left(\frac{V_{R_2H_2}}{RT} (\delta_{R_2H_2} - \bar{\delta})^2 + \ln \left(\frac{V_{R_2H_2}}{V_m} \right) + 1 + \left(\frac{V_{R_2H_2}}{V_m} \right) \right)}{c_{tot} V_{ISO} \gamma_{R_2H_2}^0} \quad (17)$$

and

$$\gamma_{ZnR_2RH} = \frac{\exp \left(\frac{V_{ZnR_2RH}}{RT} (\delta_{ZnR_2RH} - \bar{\delta})^2 + \ln \left(\frac{V_{ZnR_2RH}}{V_m} \right) + 1 + \left(\frac{V_{ZnR_2RH}}{V_m} \right) \right)}{c_{tot} V_{ISO} \gamma_{ZnR_2RH}^0} \quad (18)$$

with

$$c_{tot} = \frac{1}{V_{ISO}} + c_{ZnR_2RH} \left(1 - \frac{V_{ZnR_2RH}}{V_{ISO}} \right) + c_{R_2H_2} \left(1 - \frac{V_{R_2H_2}}{V_{ISO}} \right). \quad (19)$$

The nonidealities of the aqueous phase were calculated via activity coefficient of zinc with the Pitzer-Model taking account of the binary and ternary interaction parameters as given by the EFCE.²² Previous modeling results of multi-component diffusion coefficients and the comparison between the modeling and experimental results of activity coefficients for the investigated zinc-D2EHPA system, have been reported by Altunok.¹⁹

Figure 2 shows the calculated diffusion coefficients of zinc-D2EHPA complex depending on the zinc concentration and the initial D2EHPA concentration in the organic phase. The diffusion coefficient of zinc-D2EHPA complex decreases when either the concentration of initial D2EHPA or the zinc-D2EHPA complex increases. Calculated diffusion coefficients of zinc-D2EHPA complex in infinite diluted solution are $2.9 \times 10^{-10} \text{ m}^2/\text{s}$ for 10 wt % D2EHPA and $3.1 \times 10^{-10} \text{ m}^2/\text{s}$ for 5 wt % D2EHPA. Mörters and Bart³⁹ give the diffusion coefficient of the zinc-D2EHPA complex between 3.49 and $3.74 \times 10^{-10} \text{ m}^2/\text{s}$ for a D2EHPA concentration range of 2.6–8.5 wt % and for an initial zinc concentration range of 0.1–10 mmol/l. These results are in good agreement with the calculated diffusions coefficient of zinc-D2EHPA complex in Figure 2.

Experimental

Materials

Table 1 shows the components used for the experiments. Deionized water was used for the continuous aqueous phase. Zinc sulfate monohydrate and sulfuric acid were purchased from Merck. D2EHPA (Di-(2-ethyl hexyl)-phosphoric acid) and isododecane were kindly provided by Bayer AG, Leverkusen and EC Erdölchemie, Cologne, respectively.

The solubility of isododecane and water in each other is practically insignificant. However, to eliminate this effect, water and isododecane were saturated into each other before starting the experiments. The desired concentrations of zinc and sulfuric acid in the continuous aqueous phase and of D2EHPA in the dispersed organic phase were generated using a laboratory scale (ARC 120, OHAUS, Gießen) with a standard deviation of 0.01%. The droplets always consisted of the organic phase, which was saturated with water. The aqueous zinc concentration is analyzed by titration with EDTA (ethylene diamine tetra acetate, Merck, Darmstadt). The procedure for the analysis of the zinc by a titration in aqueous phases is described by Klocker.⁴⁰ With this method, zinc concentrations can be determined with an accuracy of $\pm 2\%$. The zinc concentration in the organic phase was analyzed externally either at the Department of Technical Chemistry-A of the University Dortmund or at the Institute for Environmental Engineering (ISA) of RWTH Aachen

Table 1. Components Used

| Product | Source | Quality |
|--|-------------------------|-----------------|
| Isododecane | EC Erdölchemie, Germany | Technical grade |
| D2EHPA | Bayer AG, Germany | Baysolvex, p.a. |
| Water | AVT | Deionized |
| Sulfuric acid | Merck KgaA, Germany | 95–97 wt % p.a. |
| ZnSO ₄ ·H ₂ O (powder) | Merck KgaA, Germany | p.a. |

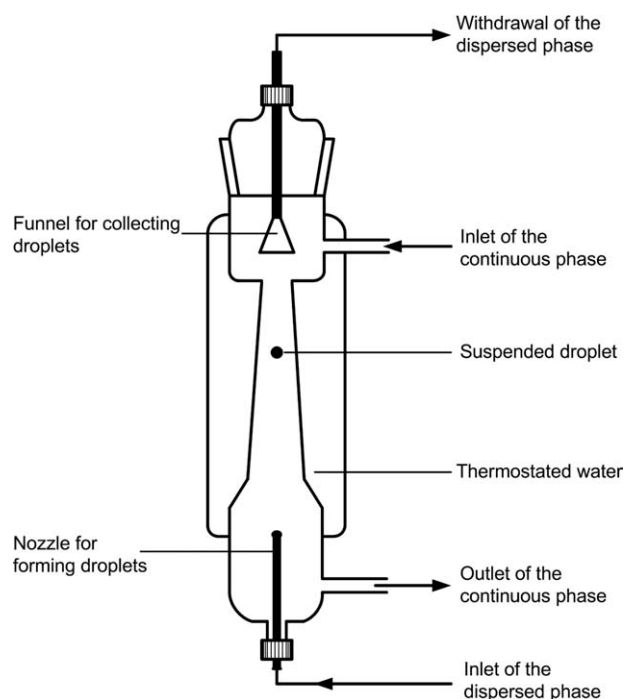


Figure 3. Mass transfer cell on lab-scale.

University by using the ICP method (Inductive Coupled Plasma, ICP-OES, Perkin-Elmer, Optima 5000DV). The device was calibrated before each measurement and controlled with blind samples. Each sample was measured three times diluted with water, e.g., 1:10, 1:100 and 1:1000. This method has a deviation of 3%. The pH of the aqueous phase was measured by a pH meter (Metrohm Herisau, model E520, Switzerland). After calibration with standard buffer solutions, a precision of ± 0.05 in the pH was reached.

Experimental setup

Experiments were performed in a lab-scale mass transfer cell as shown in Figure 3, which has been designed in a collaboration between AVT at RWTH Aachen University and Bayer Technology Services.⁴¹⁻⁴³ The used mass transfer cell has a conical segment in the mass transfer zone. The idea of using a cell with conical part, in order to ensure long contact times, was introduced by Schügerl et al.⁶

This mass transfer cell allows the determination of the mass transfer behavior of liquid systems under defined operation conditions. The mass transfer cell is made of glass. Other parts of the device consist of glass, teflon and stainless steel in order to minimize the influence of contaminants.

Figure 4 shows the experimental setup. The mass transfer cell and vessel (V) are equipped with a temperature jacket. The temperature of the continuous phase is controlled by the help of a separate heat exchanger. The temperature is measured online with a thermometer Pt 100 (TCM) and can be controlled by a thermostat (Lauda Ultra, NB-S15/12, $\pm 0.1^\circ\text{C}$, Lauda-Königshofen). The continuous phase is pumped from the vessel with a gearwheel pump (VDE 0530, VEM Motors GmbH, Thurn) via a heat exchanger to the top of the mass transfer cell. The mass flow is controlled

through a continuously adjustable mechanism. The surge tank on the top ensures the protection against overflowing and enables to vent the device during start-up. A teflon tube connects the Hamilton dosing device (Macrolab M, Hamilton, Switzerland) to the nozzles.

Glass nozzles with inner diameters of 1.3 mm and 2.2 mm were used for the generation of the single-droplets having diameters of 3.22 mm and 5 mm. A defined volume of the organic phase is ejected from the nozzle using a precision syringe (TLLX, Hamilton, Switzerland). A generated droplet rises in the surrounding continuous phase. Once the pump for the counter flow of continuous phase is turned on, the droplet is levitated in the conical part of the cell. The operation of the syringe drivers and the adjustment of the velocity of the counter-current were controlled by a personal computer with the software Visual Designer (Intelligent Instrumentation GmbH, Leinfelden-Echterdingen). With the widely automated device used it is possible to form single droplets having an exact volume without any secondary-droplet formation.

The conical part of the cell has a length of 75 mm and the diameter ranges between 20 mm at the bottom and 10 mm at the top. The velocity of the countercurrent phase varies over the conical part of the cell due to the variations in diameter. The droplet levitates at the position in the conical part where a balance between the lifting and velocity forces takes place. Cylindrical cells are not appropriate for the systems with low kinetic constants such as zinc-D2EHPA system, because in such cells the contact time between droplets and continuous phase is limited by the length of the cylindrical cells.

Each generated droplet was kept levitated throughout a specific contact time. Then the continuous phase was turned off, so that the droplet could rise and reach a funnel at the top of the cell, where they coalesce with their main phase. The same volume of the generated droplet volume was withdrawn by the help of a second precision syringe (Macrolab M, Hamilton, Switzerland). The relative maximum error in

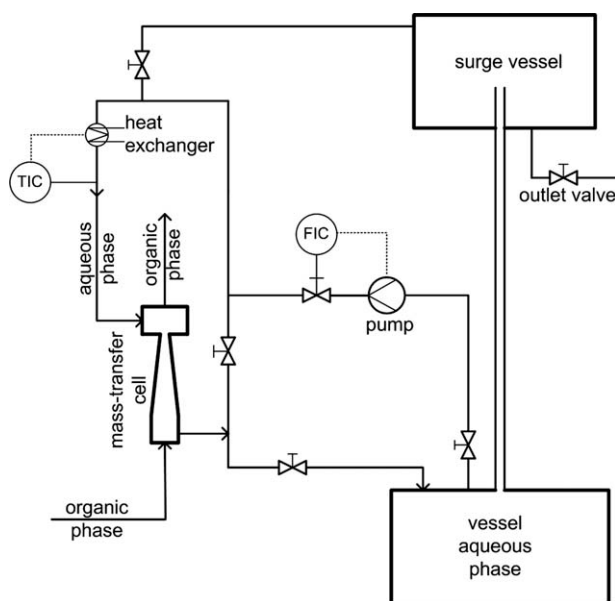


Figure 4. Experimental setup.

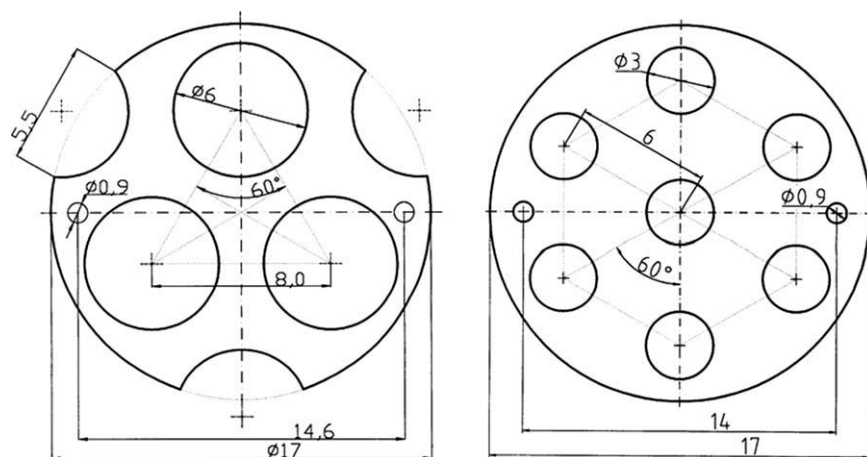


Figure 5. Tantalum sieve trays used.

the drop volume is 1.5%. Each experiment was performed twice under identical conditions to make sure that the reproducibility is maintained, which was checked analytically for both samples. Approximately 5 ml of the sample is required for analysis of zinc concentration in the organic phase. Depending on the droplet diameter, about 1040 droplets with a diameter of 3.22 mm and 300 droplets of 5 mm are required for one experimental point. The time required for an experimental point, e.g., with droplets of 3.22 mm diameter and for 60 s contact time is about 17.5 hours, excluding the time required for the start-up of the mass transfer device. This time was the realized maximum experimental duration.

For the determination of the sieve-tray influence on mass transfer, sieve trays (s. Figure 5) were installed in the mass transfer cell. The first sieve tray has a hole diameter of 6 mm and a sieve aperture ratio of 49% and the second sieve tray has a hole diameter of 3 mm and a sieve aperture ratio of 26%. During the experiments with sieve trays, the velocity of counter-current was adjusted such that the single droplets could be kept levitated underneath the installed sieve tray for a defined time interval. Afterwards the counter-current was turned off for a short time, so that the droplet could rise through the sieve tray. Following this, the counter-cur-

rent was turned on again to keep the droplet levitated above the sieve tray for a second specified time interval.

Theoretical and Experimental Results

The mass transfer of zinc in the continuous aqueous phase with D2EHPA in the dispersed organic phase was investigated in the described mass transfer cell. During the experiments, concentrations of D2EHPA, zinc, sulfuric acid, contact time, droplet diameter and diameter of sieve tray hole were varied. The theoretical and experimental results of mass transfer rate of the zinc in the organic droplets y^+

$$y^+ = \frac{y^* - y(t)}{y^* - y_0}, \quad (20)$$

are depicted in the Figures 6–10. The experimental results are summarized in Tables 2–4. The initial zinc concentration in the organic droplets (y_0) was equal zero, because the organic phase does not contain any zinc at the start of the experiments performed here. The symbols in the Figures 6–10 represent the experimental results for y^+ and the lines are the modeling results with fitted instability parameter C_{IP} for the zinc-

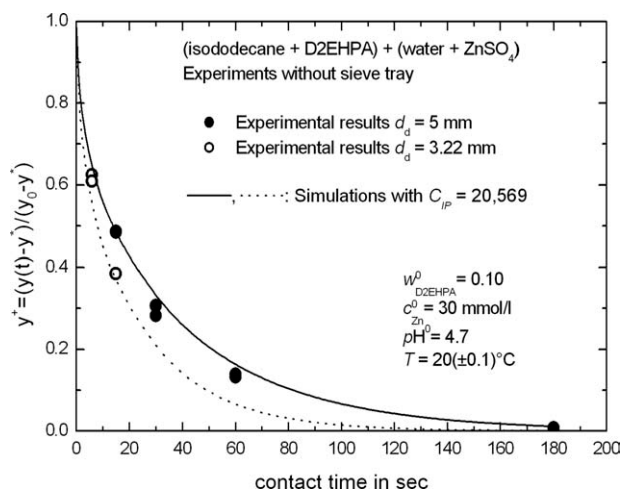


Figure 6. Mass transfer of zinc for 10 wt % D2EHPA.

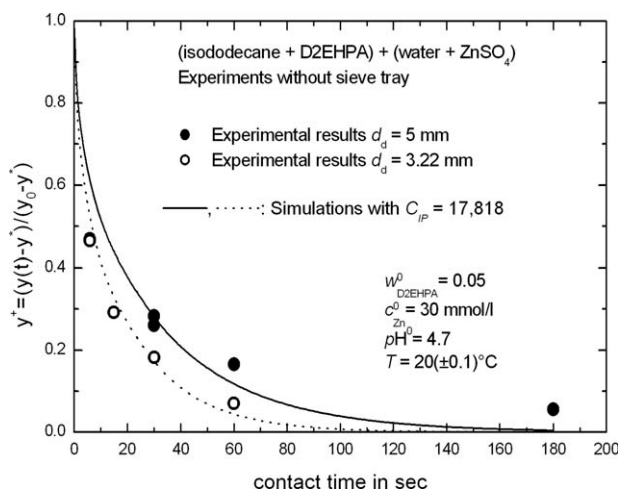


Figure 7. Mass transfer of zinc for 5 wt % D2EHPA.

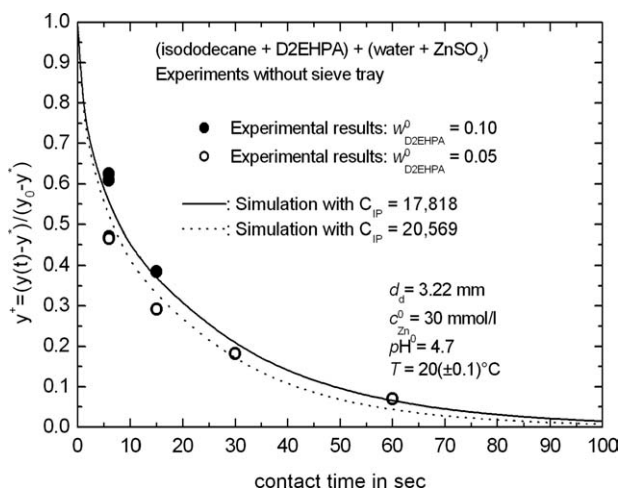


Figure 8. Effect of D2EHPA concentration on the mass transfer.

D2EHPA system. D_{eff} in the Eq. 6 takes into account the mass transfer effect depending on droplet diameter, viscosity of both phases and hydrodynamic behavior. The results of the hydrodynamic behavior of the zinc-D2EHPA system, related to thermo-physical data and internal circulation were used from Kalem et al.²⁰ Diffusion coefficients of zinc-D2EHPA complex in the organic phase were calculated with the Eq. 12, taking into account the thermodynamic factor in Eq. 13.

Figures 6 and 7 show that the droplets with smaller diameters of 3.22 mm reach equilibrium faster than the droplets with diameters of 5 mm. This is as expected, since the droplets with smaller diameter have larger volume specific surface area for the mass transfer. Furthermore the diffusion length in the small droplets is shorter.

The fitted instability parameter C_{IP} is 17818 for 5 wt % D2EHPA and 20569 for 10 wt % D2EHPA in the organic phase. Mörters and Bart³⁹ give the value of C_{IP} for the zinc-D2EHPA system as 18,636,[†] which is also in good agreement with the experimental results of this work. The dependence of the C_{IP} on the initial D2EHPA concentration can be expressed with

$$C_{\text{IP}} = 15096.36 + 54425.8 \lambda w_{\text{D2EHPA}}^0 \quad (21)$$

After the determination of the effects of the droplet diameter, the effect of the D2EHPA concentration on the mass transfer is depicted in the Figure 8 for a constant droplet diameter. By changing the D2EHPA concentration from 5 to 10 wt %, it is shown that the equilibrium is reached slower with increasing D2EHPA concentration for droplets of identical diameter. A reason for this may be the higher viscosity of the organic phase for 10 wt % D2EHPA in isododecane as compared to the system with 5 wt % D2EHPA. This effect indicates that the mass transfer rate of the zinc-D2EHPA system is limited by the diffusion of the zinc complex in the droplets.

For the experiments with sieve trays a droplet diameter of 3.22 mm was chosen. The total contact time (t) is equal to the sum of time underneath the sieve tray with droplet generation (t_u) and time above the sieve tray with withdrawal of the droplet (t_a), i.e.

[†]The value for C_{IP} as 9.1, which is divided by the constant of 2048 in Eq.5

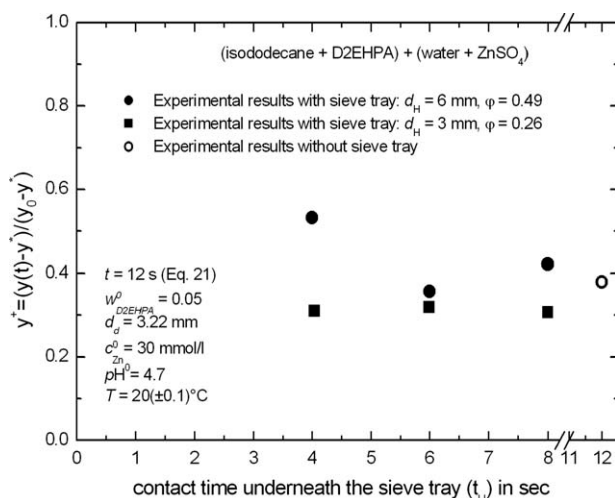


Figure 9. Sieve tray effect on the mass transfer.

$$t = t_u + t_a \quad (22)$$

The results of the experiments are shown in Figure 9. During the experiments the total contact time (t) was kept constant at 12 s, while time underneath and above the sieve tray was varied. Figure 9 shows the mass transfer rate as a function of the contact time underneath the sieve tray for 5 wt % D2EHPA in isododecane. Additionally, experiments without sieve trays were investigated as well, in order to determine the influence of sieve tray on the mass transfer rate. It can clearly be seen that with decreasing hole diameter of the sieve tray, mass transfer rate increases significantly. This is due to the increased internal mixing of droplets with 3.22 mm through the smaller sieve hole of 3 mm. The internal mixing improves the mass transfer rate through increased radial concentration distribution in the droplet. This effect is smaller for the sieve tray with the hole diameter of 6 mm. The same conclusion also applies for the physical test system of toluene + acetone + water as reported by Henschke,³ who found a mass transfer

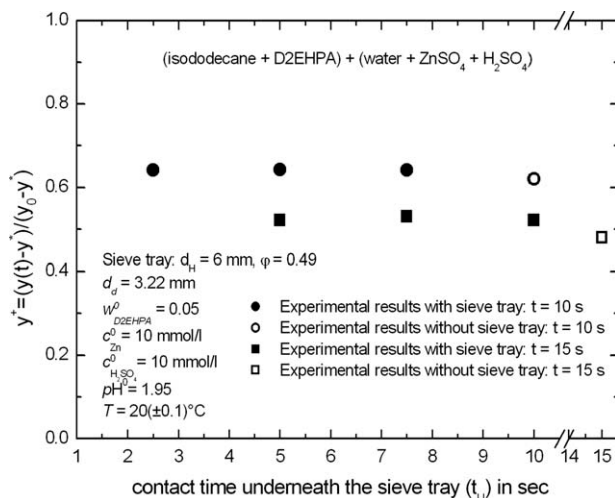


Figure 10. Sieve tray effect on the mass transfer with sulfuric acid.

Table 2. Experiments Without Sieve Tray for a Start Concentration of 30 mmol/l Zinc in the Aqueous Phase ($\text{pH}^0 = 4.7$, $c_{\text{H}_2\text{SO}_4} = 0$)

| W_{D2EHPA} (%) | d_d (mm) | t (s) | y (ppm) | y^* (ppm) | y^+ (—) |
|-------------------------|------------|---------|-----------|-------------|-----------|
| 5 | 3.22 | 6 | 2142.2 | 4000 | 0.4645 |
| 5 | 3.22 | 6 | 2136.6 | 4000 | 0.4659 |
| 5 | 3.22 | 15 | 2832.8 | 4000 | 0.2918 |
| 5 | 3.22 | 15 | 2830.2 | 4000 | 0.2925 |
| 5 | 3.22 | 30 | 3269.7 | 4000 | 0.1826 |
| 5 | 3.22 | 60 | 3720.5 | 4000 | 0.0699 |
| 5 | 5.0 | 30 | 2869.0 | 4000 | 0.2828 |
| 5 | 5.0 | 30 | 2957.3 | 4000 | 0.2607 |
| 5 | 5.0 | 60 | 3336.9 | 4000 | 0.1658 |
| 5 | 5.0 | 180 | 3778.0 | 4000 | 0.0555 |
| 10 | 3.22 | 6 | 2614.1 | 6960 | 0.6244 |
| 10 | 3.22 | 6 | 2721.7 | 6960 | 0.6090 |
| 10 | 3.22 | 15 | 4281.1 | 6960 | 0.3849 |
| 10 | 5.0 | 15 | 3578.8 | 6960 | 0.4858 |
| 10 | 5.0 | 30 | 4828.0 | 6960 | 0.3063 |
| 10 | 5.0 | 30 | 4994.1 | 6960 | 0.2825 |
| 10 | 5.0 | 60 | 6036.9 | 6960 | 0.1326 |
| 10 | 5.0 | 60 | 5996.6 | 6960 | 0.1384 |
| 10 | 5.0 | 180 | 6910.1 | 6960 | 0.0072 |

enhancement of 24.7% for the toluene-acetone-droplets of 3.22 mm diameter through sieve hole of 3 mm and of 6% for the same droplet diameter through sieve holes of 6 mm. It can be seen in Figure 9 that a sieve tray with constant diameter larger than the droplet diameter does not have any significant influence on the mass transfer of the zinc with D2EHPA.

Figure 10 shows the measurements with 10 mmol/l zinc and 10 mmol/l sulfuric acid in the aqueous phase. As expected, the zinc extraction increases with increasing contact time. Furthermore, in Figure 10 it can be seen, that with decreasing pH in the aqueous phase, the extraction of zinc decreases. During the experiments the percentage of contact time underneath the installed sieve tray was varied. Even here it can be shown once more that the effect of sieve trays on zinc extraction with D2EHPA is negligible if the hole diameter is larger than the droplet diameter.

Summary and Conclusions

The mass transfer behavior of the reactive standard test system $\text{zinc}^+\text{D2EHPA}$ was investigated. Experiments were carried out with and without sieve trays of different hole diameters. Droplet diameter, contact time, concentration of cation exchanger D2EHPA, zinc and sulfuric acid were varied. In the experiments without sulfuric acid the zinc concentration was kept constant at 30 mmol/l, and 10 mmol/l in the experiments with sulfuric acid.

Table 3. Experiments with Sieve Tray for a Start Concentration of 30 mmol/l Zinc in the Aqueous Phase ($\text{pH}^0 = 4.7$, $c_{\text{H}_2\text{SO}_4} = 0$)

| W_{D2EHPA} (%) | d_d (mm) | $d_{\text{H-ST}}$ (mm) | t (s) | t_a (s) | t_u (s) | y (ppm) | y^* (ppm) | y^+ (—) |
|-------------------------|------------|------------------------|---------|-----------|-----------|-----------|-------------|-----------|
| 5 | 3.22 | Without | 12 | — | — | 3460 | 5540 | 0.38 |
| 5 | 3.22 | 3 | 12 | 8 | 4 | 3820 | 5540 | 0.31 |
| 5 | 3.22 | 3 | 12 | 6 | 6 | 3770 | 5540 | 0.32 |
| 5 | 3.22 | 3 | 12 | 4 | 8 | 3840 | 5540 | 0.31 |
| 5 | 3.22 | 6 | 12 | 8 | 4 | 2590 | 5540 | 0.53 |
| 5 | 3.22 | 6 | 12 | 6 | 6 | 3560 | 5540 | 0.36 |
| 5 | 3.22 | 6 | 12 | 4 | 8 | 3200 | 5540 | 0.42 |

Table 4. Experiments with Sieve Tray for a Start Concentration of 10 mmol/l Zinc and 10 mmol/l H_2SO_4 in the Aqueous Phase ($\text{pH}^0 = 1.95$)

| W_{D2EHPA} (%) | d_d (mm) | $d_{\text{H-ST}}$ (mm) | t (s) | t_a (s) | t_u (s) | y (ppm) | y^* (ppm) | y^+ (—) |
|-------------------------|------------|------------------------|---------|-----------|-----------|-----------|-------------|-----------|
| 5 | 3.22 | Without | 10 | — | — | 840 | 2210 | 0.62 |
| 5 | 3.22 | 6 | 10 | 7.5 | 2.5 | 794 | 2210 | 0.64 |
| 5 | 3.22 | 6 | 10 | 5 | 5 | 792 | 2210 | 0.64 |
| 5 | 3.22 | 6 | 10 | 2.5 | 7.5 | 793 | 2210 | 0.64 |
| 5 | 3.22 | Without | 15 | — | — | 1150 | 2210 | 0.48 |
| 5 | 3.22 | 6 | 15 | 10 | 5 | 1060 | 2210 | 0.52 |
| 5 | 3.22 | 6 | 15 | 7.5 | 7.5 | 1040 | 2210 | 0.53 |
| 5 | 3.22 | 6 | 15 | 5 | 10 | 1060 | 2210 | 0.52 |

As expected, mass transfer proceeds with increasing contact time. For constant D2EHPA concentrations, the equilibrium is reached faster, when the droplet diameter decreases. Interestingly with increasing D2EHPA concentration the mass transfer rate in the droplets decreases. This indicates that the mass transfer rate in the droplets is limited by the diffusion of the zinc-D2EHPA complex in the organic phase.

Modeling of the mass transfer was done using an instability parameter, which takes all transient effects during mass transfer into account. Besides temperature, the instability parameter depends on the D2EHPA and zinc concentrations but is not a function of either droplet diameter or contact time. The C_{IP} is a substance specific constant, which takes into account transient effects at the interface, e.g., through interfacial turbulence. The dependence of the mass transfer on droplet diameter, on hydrodynamic and viscosity of phases are covered by the effective diffusion coefficient D_{eff} .

The effect of the zinc concentration and pH shift on the viscosity of the aqueous phase is negligible. The viscosity of the organic phase was calculated depending on the D2EHPA concentration as described by the EFCE.²² Diffusion coefficients of zinc-D2EHPA complex in the organic phase were calculated according to the Wilke-Chang-Model³⁷ under consideration of thermodynamic factor with the Darken-Model.³⁸ The activity coefficient of zinc in the aqueous phase was calculated after Pitzer-Model,^{19,40,44} and the activity coefficient of D2EHPA in the organic phase after the Hildebrand-Scott theory.⁴⁵ The hydrodynamic effects on the mass transfer were taken into account via sedimentation velocities, depending on the thermo physical data, diameter and internal circulation of the droplet. The sedimentation velocities (v_∞) of the zinc-D2EHPA system were used as reported by Kalem et al.²⁰ All experiments were carried out at the temperature of 20°C. The temperature effect on reaction and mass transfer mechanism were not investigated in this work.

Although the order of magnitude of C_{IP} and that of diffusion coefficients are similar to those reported earlier by Morter and Bart,³⁹ the variation in numbers is almost 10%. With a constant C_{IP} value it is not possible to obtain sufficient results to describe the mass transfer behavior over a broad concentration range of D2EHPA and zinc.³⁹ A sensitivity analysis showed that a variation of C_{IP} value by 10% results in a concentration profile deviation of 29% for 5 wt % D2EHPA and of 13% for 10 wt % D2EHPA. Thus, for a reliable modeling results C_{IP} should be determined for desired concentrations of zinc and D2EHPA. The additional convection (eddy diffusion) of free moving droplets seems to

be well covered by the instability parameter, if this is fitted to the experiments at the desired temperature and desired concentration of zinc and D2EHPA. Modeling of the mass transfer with instability parameters, including all transient effects besides kinetics, allows technically usable and easily applicable results. This is shown by the close agreement between the experimental and simulation results.

Experiments with sulfuric acid show that the mass transfer of zinc into the organic droplets decreases with increasing concentration of H^+ in the aqueous phase. Furthermore, the experiments with sieve trays demonstrate that the mass transfer of zinc can be increased significantly by decreasing sieve hole diameter, whereas the mass transfer is not further improved for a sieve tray with a hole diameter larger than the droplet diameter.

Notation

a_i = model parameter
 C_{IP} = instability parameter
 c = molar concentration, mol/l
 d = diameter, m
 D = diffusion coefficient, m^2/s
 Fo = Fourier number
 K = equilibrium constant
 M = molar mass, g/mol
 R = gas constant, J/(K mol)
 RH = D2EHPA monomer
 R_2H_2 = D2EHPA dimer
 t = time, s
 T = temperature, °C
 v = velocity, m/s
 V = molar volume, m^3/mol
 w = weight percent, %
 wt = weight
 y = mass concentration in droplet phase
 ZnR_2RH = zinc-D2EHPA complex

Greek letters

δ = Kronecker delta
 φ = association parameter
 Γ = thermodynamic factor
 γ = activity coefficient
 η = viscosity, Pa s

Subscripts

a = above
 eff = effective
 d = droplet, dispersed
 c = continuous
 H = hole
 ISO = isododecane
 ST = sieve tray
 u = underneath
 tot = total
 ∞ = in infinitely extended fluid
 0 = initial

Superscripts

0 = at infinite dilution
 * = equilibrium
 I = interface

Literature Cited

1. Cox M, Hidalgo M, Valiente, M, editors. Solvent Extraction for the 21st Century, In: *Proceedings of the ISEC'99, 1+2, Society of Chemical Engineering (SCI)*, London, 2001:1–1680.

2. Henschke M, Pfennig A. Auslegung von Siebbodenkolonnen für die Flüssig/Flüssig Extraktion auf der Basis von einfachen Laborversuchen. *Chem Ing Tech.* 2000;72:964–965.
3. Henschke M. *Auslegung pulsierter Siebboden-Extraktionskolonnen*. Aachen: Shaker Verlag, 2003.
4. Bart HJ, Garthe D, Grömping T, Pfennig A, Schmidt S, Stichmaier J. Vom Einzeltropfen zur Extraktionskolonne. *Chem Ing Tech.* 2006;78:543–547.
5. Pilhofer T, Mewes, D. *Siebboden-Extraktionskolonnen*. Weinheim: Verlag Chemie, 1979.
6. Schügerl K, Hänsel R, Schlichting E, Halwachs WR. *Chem Ing Tech.* 1986;58:308–317.
7. Reschke M. Reaktivextraktion von Penicillin. Doctoral Thesis, University of Hannover, 1983.
8. Schügerl K. *Solvent Extraction in Biotechnology, Recovery of Primary and Secondary Metabolites*. Berlin: Springer Verlag, 1994.
9. Ji, J, Mensforth, KH, Perera, JM, Stevens, GW. The role of kinetics in the extraction of zinc with D2EHPA in a packed column. *Hydrometallurgy* 2006;84:139–148.
10. Attarakih MM. Solution methodologies for the population balance equations describing the hydrodynamics of liquid-liquid-extraction. Doctoral Thesis, Technical University of Kaiserslautern, 2004.
11. Attarakih MM, Bart HJ, Faqir, NM. Numerical solution of the bivariate population balance equation for the interacting hydrodynamics and mass transfer in liquid-liquid extraction columns. *Chem Eng Sci.* 2005;60:1–12.
12. Schmidt SA, Tagnen M, Attarakih MM, Lagar GL, Bart HJ. Droplet population balance modelling-hydrodynamics and mass transfer. *Chem Eng Sci.* 2006;61:246–256.
13. Arimont K, Soika M, Henschke M. Simulation einer pulsierten Füllkörperextraktionskolonne. *Chem Ing Tech.* 1996;68:276–279.
14. Henschke M, Pfennig A. Simulation of packed extraction columns with the REDROP model. Presented at the 12th International Congress of Chemical and Process Engineering, Chisa, Praha, Czech Republic, August 25–30, 1996.
15. Arimont K. *Berechnung des Extraktionsprozesses in pulsierten Füllkörperkolonnen, Fortschritt-Berichte VDI, Reihe 3, Nr. 482*, VDI-Verlag Düsseldorf, 1997.
16. Weber M, Bäcker W, Grömping T, Pfennig A. Anwendung der neuen Auslegungsmethode für Extraktionskolonnen auf ein technisches Beispiel, 589. DECHEMA-Kolloquium am 10. März 2005, DECHEMA-Haus, Frankfurt am Main, 2005.
17. Altunok M, Grömping T, Pfennig A. Prediction of extraction-column behaviour based on lab scale experiments. Presented at the International Solvent Extraction Conference, ISEC 2005, 19–23 September, Beijing, China, 2005.
18. Altunok M, Grömping T, Pfennig A. ReDrop—an efficient tool for describing solvent and reactive extraction columns. *Comp Aid Chem Eng Part A.* 2006;21:665–670.
19. Altunok M. *Zur Auslegung von Siebbodenextraktionskolonnen für die Reaktivextraktion basierend auf Versuchen im Labormaßstab, Reihe 3, Nr. 905*. Düsseldorf: VDI Verlag, 2009.
20. Kalem M, Altunok M, Pfennig, A. Sedimentation behavior of droplets for the reactive extraction of zinc with D2EHPA. *AIChE J.* 2010;56:160–167.
21. Mivsek M, Berger B, Schröter J. *Standard test systems for liquid extraction. The Institution of Chemical Engineers, 2. Auflage*. Warwickshire: EFCE Publications Series 46, 1985.
22. Bart HJ, Slater MJ. Standard test system for reactive extraction-zinc/D2EHPA, European Federation of Chemical Engineering (EFCE), 2001. Available online at: http://www.processnet.org/processnet_media/FG+Fluidynamik+und+Trenntechnik/Extraktion/EFCE_Testsysteme.pdf.
23. Hancil V, Slater MJ, Yu W. On the possible use of di-(2-ethylhexyl) phosphoric acid/Zinc as a recommended system for liquid-liquid extraction: the effect of impurities on kinetics. *Hydrometallurgy* 1990;63:375–386.
24. Sainz-Diaz CI, Klocker H, Marr R, Bart HJ. New approach in the modelling of the extraction equilibrium of Zinc with bis-(2-ethylhexyl) phosphoric acid. *Hydrometallurgy* 1996;42:1–11.
25. Bart HJ. *Reactive extraction*. In: Mewes D, Mayinger F, editors. *Heat and Mass Transfer*. Heidelberg: Springer, 2001.
26. Newman AB. The drying of porous solids: diffusion and surface emission equations. *AIChE J.* 1931a;27:203–220.
27. Newman AB. The drying of porous solids: diffusion calculation. *AIChE J.* 1931b;27:310–333.

28. Kronig R, Brink JC. On the theory of extraction from falling droplets. *Appl Sci Res*. 1950;A2:142–154.
29. Hadamard JS. Mouvement permanent lent d'une sphere liquide et visqueuse dans un liquide visqueux. *C R Acad Sci*. 1911;152:1735–1743.
30. Rybczynski W. Über die fortschreitende Bewegung einer flüssigen Kugel in einem zähen medium. *Bull Int Acad Sci Cracovie Ser A*. 1911;40:40–46.
31. Handlos AE, Baron T. Mass and heat transfer from drops in liquid-liquid extraction. *AIChE J*. 1957;3:127–136.
32. Sawitowski H. *Interfacial phenomena*. In: Hanson C, editor. *Recent Advances in Liquid-Liquid Extraction*. Oxford: Pergamon Press, 1971.
33. Pfennig A. Mass transfer across an interface induces formation of mikro droplets in lattice systems. *Chem Eng Sci*. 2000;55:5331–5337.
34. Yurtov EV, Koroleva MY, Golubkov AS, Gregorjev WB. Strukturmechanische barrieren bei der membranextraktion mit mehrkomponenten-emulsionen. *Dokl Akad Nauk*. 1988;302:1164.
35. Henschke M, Pfennig A. Mass-transfer enhancement in single-drop extraction experiments. *AIChE J*. 1999;45:2079–2086.
36. Henschke M, Pfennig A. Influence of sieve trays on the mass transfer of single droops. *AIChE J*. 2002;48:227–234.
37. Wilke CR, Chang P. Correlation of diffusion coefficients in dilute solutions. *AIChE J*. 1995;1:264–270.
38. Darken LS. Diffusion, mobility and their interrelation through free energy in binary metallic systems. *Trans Am Inst Mining Metall Eng*. 1948;175:184–201.
39. Mörters M, Bart HJ. Mass transfer into droplets undergoing reactive extraction. *Chem Eng Proc*. 2003;42:801–809.
40. Klocker H. Multikomponentenstoffaustausch bei der reaktivextraktion im system zinksulfat/di(2-ethylhexyl)phosphorsäure. PhD thesis, Technical University Graz, Austria, 1996.
41. Vollmari G. Entwicklung einer messzelle zur ermittlung der kinetik des stoffübergangs in dispersen flüssig-flüssig-systemen. Diploma thesis, Aachener Verfahrenstechnik, RWTH Aachen University, 1993.
42. Schliefer S. Untersuchungen zum stoffaustauschverhalten von einzel-tropfen unter einfluss der fluiddynamik. Diploma thesis, Aachener Verfahrenstechnik, RWTH Aachen University, 1996.
43. Schröter J, Bäcker W, Hampe MJ. Stoffaustauschversuche an einzel-tropfen und in tropfenschwärmen in einer gegenstrommeßzelle. *Chem Ing Tech*. 1998;70:279–283.
44. Pitzer KS. *Activity coefficients in electrolyte solutions, Chapter 7*, Baton Rouge: CRC Press, 1979:157–208.
45. Hildebrand JH, Scott RL. *The Solubility of Nonelectrolytes*. New York: Reinhold Publishing, 1990.
46. Mivsek M, Berger B, Schröter L. *Standard Test Systems for Liquid Extraction*. The Institution of Chemical Engineers, 2nd ed. Warwickshire: EFCE Publication Series 46, 1985.

Manuscript received Aug. 23, 2010, and revision received May 1, 2011.